Article

Real-Time Multi-GNSS Precise Orbit Determination Based on the Hourly Updated Ultra-Rapid Orbit Prediction Method

Bingfeng Tan *[ID], Yunbin Yuan, Qingsong Ai [ID] and Jiuping Zha

Innovation Academy for Precision Measurement Science and Technology, Chinese Academy of Sciences, West No.30 Xiao Hong Shan, Wuhan 430071, China
* Correspondence: bingfengtan@whigg.ac.cn

Abstract: Offering real-time precise point positioning (PPP) services for global and large areas based on global navigation satellite systems (GNSS) has drawn more and more attention from institutions and companies. A precise and reliable satellite orbit is a core premise for multi-GNSS real-time services, especially for the GPS and GLONASS, which are undergoing modernization, whereas the Galileo, BDS and QZSS have just fulfilled the construction stage. In this contribution, a real-time precise orbit determination (POD) strategy for the five operational constellations based on the hourly updated ultrarapid orbit prediction method is presented. After combination of 72 h arc through three adjacent 24 h arc normal equations, the predicted orbits are finally generated (hourly updated). The POD results indicate that the mean one-dimensional (1-D) root mean square (RMS) values compared with the Deutsches GeoForschungsZentrum (GFZ) final multi-GNSS orbits are approximately 3.7 cm, 10.2 cm, 5.8 cm, 5.7 cm, 4.1 cm and 25.1 cm for GPS, BDS IGSOs, BDS MEOs, GLONASS, Galileo and QZSS NONE GEOs, respectively. The mean 1-D RMS values of the hourly updated ultrarapid orbit boundary overlapping comparison are approximately 1.6 cm, 6.9 cm, 3.2 cm, 2.7 cm, 1.8 cm and 22.2 cm for GPS, BDS IGSOs, BDS MEOs, GLONASS, Galileo and QZSS NONE GEOs, respectively. The satellite laser ranging (SLR) validation illuminates that the mean RMS values are approximately 4.53 cm and 4.73 cm for the four MEOs of BDS-3 and four BDS-2 satellites, respectively.

Keywords: real-time precise orbit determination; multi-GNSS; hourly updated; satellite laser ranging; solar radiation pressure model

1. Introduction

The US Global Positioning System (GPS) and the Russian GLObal NAvigation Satellite System (GLONASS) are going through the process of modernization nowadays. GPS constellation is composed of 32 operational satellites, including five BLOCK IIIA satellites (G04, G11, G14, G18, G23) with the capability of transmitting L2C and L5 signals. For the GLONASS constellation, there are 21 operational satellites used for navigation, including three new GLONASS-K1 satellites (R09, R11, R22) with the capability of transmitting both FDMA and CDMA signals. Meanwhile, the emerging satellite navigation systems, i.e., European Galileo Navigation Satellite System (Galileo), Chinese BeiDou Navigation Satellite System (BDS) and Japanese Quasi-Zenith Satellite System (QZSS), have just fulfilled the constellation networking phase. Concerning BDS, with a constellation consisting of four in medium earth orbit (MEO), five in inclined geosynchronous orbit (IGSO) and five in geostationary orbit (GEO), BDS-2 has been offering positioning, navigation and timing (PNT) services for the Asia-Pacific region since the end of 2012. BDS-3 has been officially providing global PNT services since 31 July 2020 with a constellation of 24 MEO, 3 IGSO and 3 GEO satellites [1,2]. With 24 full operational capability (FOC) satellites and 4 in orbit validation (IOV) satellites, Galileo has officially started offering PNT services since the end of 2016. For QZSS, four IGSO and one GEO satellites have been deployed. The

operational status of the GNSS constellations are summarized in Table 1, as of July 2022. Increasingly perfect multi-GNSS bring great potential for more reliable and precise global capable real-time PPP services [3–5].

Table 1. Operational status of the GNSS constellations as of July 2022.

System	Type	Signals	Sats
GPS	Block IIR	L1 C/A, L1/L2 P(Y)	8
	Block IIR-M	L1 C/A, L1/L2 P(Y), L2C, L1/L2 M	7
	Block IIF	L1 C/A, L1/L2 P(Y), L1/L2 M, L2C, L5	12
	Block IIIA	L1 C/A, L1/L2 P(Y), L1/L2 M, L2C, L5	5
GLONASS	GLONASS-M	L1/L2 C/A and P, L3, FDMA	18
	GLONASS-K1	L1/L2 C/A and P, L3, FDMA+CDMA	3
BDS-2	GEO	B1I, B2I, B3I	5
	IGSO		7
	MEO		3
BDS-3	GEO	B1C, B2a, B2b, B3C, B1I, B3I	3
	IGSO		3
	MEO		24
Galileo	IOV	E1, (E6), E5a/b/ab	4
	FOC		24
QZSS	GEO	L1 C/A (L1 C/B), L1-SAIF, L1C, L2C, L5, L6-LEX	1
	IGSO		4

High-accuracy, stable real-time GNSS satellite orbit and clock corrections are the footstone for real-time PPP and PPP-RTK applications [6–12], especially satellite orbits. Ultrarapid orbit determination and real-time filtering are the two prevailing methods for GNSS satellite real-time POD. POD based on the real-time filtering method has drawn increasing attention from research institutes and commercial companies. Jet Propulsion Laboratory (JPL) developed the real-time GIPSY (RTG) software using a square root information filter (SRIF). RTG has been employed in many real-time service systems with an accuracy of 5 cm for the user range error (URE) as of 2020 [13]. Auto-BAHN was developed by Newcastle University by using an extended Kalman filter (EKF) [14]. The Kalman filtering algorithm was also used by Centre National D'Etudes Spatiales (CNES) for multi-GNSS orbit and clock estimation [15]. Multi-GNSS Advanced Demonstration Tool for Orbit and Clock Analysis (MADOCA) was developed by Japan using the EKF method, and then employed for providing augmentation services for QZSS [16]. Dai et al. [17] and Duan et al. [18] have also done some research on filtering POD of multi-GNSS constellations.

Currently, several Multi-GNSS Experiment (MGEX) [19] and International GNSS Monitoring and Assessment System (iGMAS) [20] analysis centers have provided multi-GNSS ultrarapid orbit products or demonstrated their processing systems, e.g., GFZ [21], Wuhan University [22–25], Innovation Academy for Precision Measurement Science and Technology (APM, CAS) and Shanghai Astronomical Observatory (SHAO, CAS). Wuhan University [26], GFZ and SHAO have also demonstrated their hourly ultrarapid multi-GNSS satellite orbits. Ultrarapid orbits have been widely used in the International GNSS Service (IGS) Real Time Service (RTS), which was formally launched in 2013 [27–29]. The RTS currently provides a GPS-only service. Multi-GNSS orbit and clock products are undergoing development and testing phases, including a number of streams from analysis centers and an experimental combination solution. The IGS RTS combinations, individual analysis center streams and NTRIP mountpoint designations are listed in Table 2 (https://igs.bkg.bund.de/ntrip/ppp), (accessed on 25 July 2022).

Table 2. Status of IGS RTS combinations and individual analysis center products.

Center	Description	Mountpoint
IGS01	GPS-only orbit and clock corrections based on IGS ultrarapid orbits; Single-Epoch GPS clock combination, RETINA solution	SSRA01IGS0
IGS02	GPS-only orbit and clock corrections based on IGS ultrarapid orbits; Kalman Filter GPS clock combination, BNC solution	SSRA02IGS0
IGS03	GPS+GLONASS orbit and clock corrections based on IGS ultrarapid orbits; Kalman Filter GPS+GLONASS clock combination, BNC solution	SSRA03IGS0
BKG	GPS+GLONASS orbit and clock corrections based on IGS ultrarapid orbits	SSRA00BKG0
CNES	GPS+GLONASS orbit and clock corrections based on IGS ultrarapid orbits	SSRA00CNE0
CAS	GPS+GLONASS orbit and clock corrections based on internal ultrarapid orbits	SSRA00CAS0
DLR/GSOC	GPS+GLONASS orbit and clock corrections based on IGS ultrarapid orbits	SSRA00DLR0
ESA/ESOC	GPS-only orbit and clock corrections based on IGS ultrarapid orbits	SSRA00ESA0
	GPS-only orbit and clock corrections based on internal ultrarapid orbits	SSRA01ESA0
GFZ	GPS+GLONASS orbit and clock corrections based on IGS ultrarapid orbits	SSRA00GFZ0
GMV	GPS+GLONASS orbit and clock corrections based on internal ultrarapid orbits	SSRA00GMV0
NRCan	GPS-only orbit and clock corrections using NRT batch orbits every hour (APC)	SSRA00NRC0
SHAO	GPS+GLONASS orbit and clock corrections based on internal ultrarapid orbits	SSRA00SHA0
WUHAN	GPS+GLONASS orbit and clock corrections based on IGS ultrarapid orbits	SSRA00WHU0

APM (which was former called Institute of Geodesy and Geophysics, Chinese Academy of Sciences, CAS) has provided real-time orbit and clock streams to IGS RTS since 2020 with the mountpoint of SSRA00CAS0. In this contribution, the hourly updated ultrarapid orbit prediction strategy is described in detail. The contribution is structured as follows. The ground tracking network used to estimate the hourly updated ultrarapid multi-GNSS orbits and the POD processing strategy at APM are summarized in Section 2. Orbits are assessed by comparing with GFZ final multi-GNSS orbits, orbit boundary overlapping comparison and SLR validation, and the corresponding results are addressed and analyzed in Section 3. In Section 4, the results are further analyzed, and some key issues are discussed. Finally, a summary is made in Section 5.

## 2. Methods

2.1. GNSS Tracking Networks

2.1.1. iGMAS Tracking Network

To analyze the signals of multi-GNSS constellations, and to investigate the PNT performance of the multi-GNSS, the iGMAS has been established by China. A continuous tracking network for BDS and other GNSS satellites has been deployed by iGMAS. Up to July 2022, iGMAS comprises 21 operational stations, 8 in China and 13 abroad. All of these data collected by iGMAS tracking stations could be downloaded from the iGMAS data archive centers, e.g., Wuhan University and National Time Service Center (NTSC, CAS).

2.1.2. IGS Tracking Network

The IGS, as important component of the International Association of Geodesy (IAG), has been providing high-quality GNSS raw data for analysis centers and global research institutes. The MGEX pilot project has been established by the IGS to track and collect multi-GNSS signals, including the BDS, Galileo and QZSS systems, as well as modernized GPS and GLONASS satellites. The hourly data from about three hundred sites have been collected by the IGS data archive centers, e.g., Crustal Dynamics Data Information System (CDDIS) and Institut National de l'Information Géographique et Forestière (IGN).

In this contribution, 21 iGMAS stations and 100 IGS stations are chosen for hourly updated ultrarapid POD study, and station distribution is demonstrated in Figure 1. The observation data from 1 June 2021 to 31 May 2022 are processed.
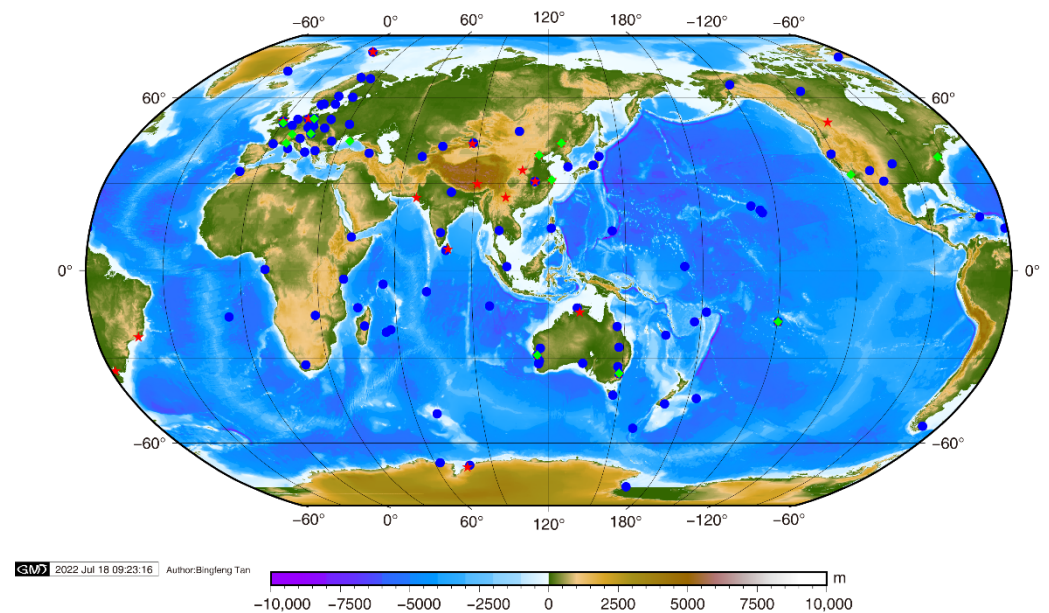

Figure 1. Tracking stations used in multi-GNSS real-time POD and SLR validation. The stations are remarked by blue circles, red five-pointed stars and green diamonds for IGS, iGMAS and SLR tracking stations, respectively.

2.2. Hourly Updated Ultrarapid POD Strategy

Nowadays, most of the IGS/MGEX/iGMAS analysis centers update their ultrarapid orbit products every 6 h or ever 3 h, few of which contain BDS, Galileo and QZSS. In order to enhance the solution accuracy and stability, an arc length of 24 h is selected, and then recent adjacent normal equations are combined up to a length of 72 h for the orbit fitting and prediction. The procedure of ultrarapid orbit determination and prediction is illuminated in Figure 2. The sliding window size is 24 h, and the arc length for each solution is 24 h shifted by 1 h. For the current solution, 24 h arc observations are processed and then combined with two existing adjacent 24 h arcs at a normal equation level to generate a 72 h solution. Finally, a 24 h orbit prediction is conducted after orbit fitting, and the predicted part of the orbit is further used by satellite clock error estimation program. Meanwhile, we proposed a station-clustered and parallel processing strategy using two identical Linux cloud servers (Operating system: CentOS Linux release 7.8, CPU 3.30 GHz, CPU cores: 8, total memory: 148,688,684 kB) to improve the computation efficiency and to ensure the accuracy and reliability of the predicted orbit. Ground tracing stations are classified into six clusters according to geographical distribution and then run in parallel at the parameter estimation stage with idle CPU cores automatically selected. Then, the six clusters are combined at the normal equation level to generate the current solution. For the 72 h combination and 24 h

prediction processing, the five-constellation POD can be conducted within one hour, and thus, hourly updated orbit is achievable.
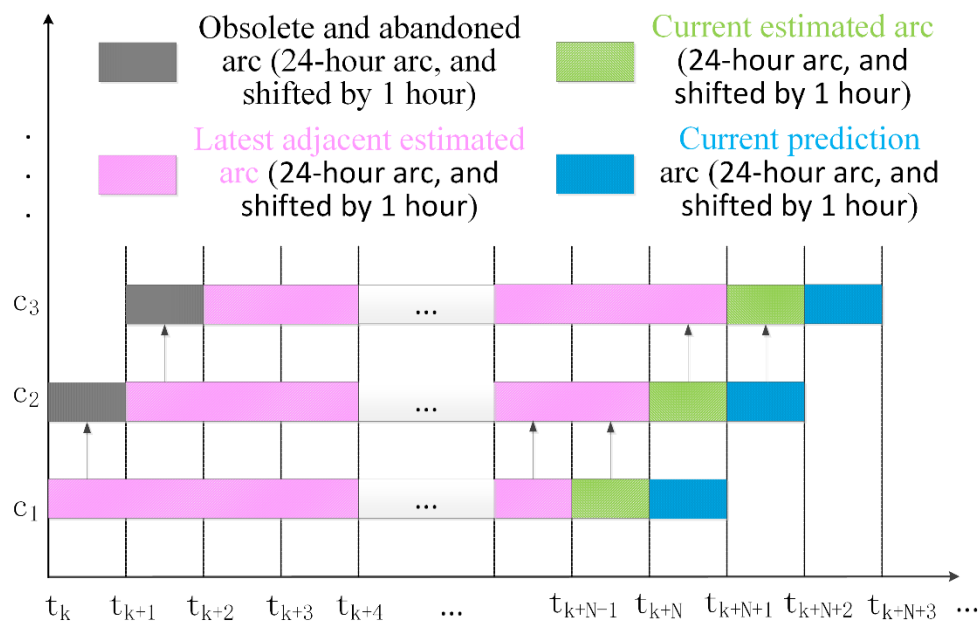
**Figure 2.** Flowchart of ultrarapid orbit determination and prediction.

The post-processing software platform, which has been developed by the analysis center of iGMAS at APM, has been adapted for ultrarapid POD processing in this contribution. Observations from five constellations have been processed simultaneously while the observational geometry for Galileo and BDS has been significantly improved. The main aspects of real-time POD processing strategy are listed in Table 3, and the procedure is summarized in Figure 3.

Table 3. Outline of the ultrarapid POD strategy for multi-GNSS.

Aspect	Summary
Observations	Double-differenced ionosphere-free phase. GPS/GLONASS/QZSS: L1, L2; BDS: B1I, B3I; Galileo: E1, E5a
Elevation angle cut-off	$7°$
Stations	21 iGMAS stations and 100 IGS/MGEX stations
Sampling rate	300 s
Data coverage	A length of 72 h arc combined through three adjacent 24 h arc normal equations
Orbits	Initial positions and velocities from broadcast ephemeris
Weighting	6 mm for phase observations with elevation-dependent weighting
Satellite antenna PCO and PCV	Satellite antenna PCOs and PCVs of GPS/GLONASS/QZSS L1/L2, Galileo E1/E5a and BDS B1I/B3I from igs14_2196.atx. For BDS and Galileo receiver antenna, the values of GPS L1/L2 have been used for the BDS B1I/B3I and Galileo E1/E5a, as their calibrations are unavailable in the igs14.atx [30]
Attitude model	GPS/GLONASS/Galileo/BDS-3: Yaw steering BDS-2/QZSS: Yaw steering + orbit normal
Troposphere	GMF mapping functions; ZTDs estimated at intervals of 2 h

Table 3. *Cont.*

Aspect	Summary
Precession and nutation	IAU 2010 model
Geopotential	EGM2008 12 × 12
Solid Earth tides, ocean tides and solid Earth pole tides	IERS Conventions 2010 [31]
N body gravitation	DE405 ephemeris from JPL
Solar Radiation Pressure (SRP) model	GPS/GLONASS/QZSS: seven-parameter ECOM2 (D1B1) BDS-2: five-parameter ECOM1 BDS-3/Galileo: cuboid a priori plus five-parameter ECOM1
Pseudo-stochastic orbit parameters	Every half day; constrained to 1×10^{-6} m/s in the radial, 1×10^{-5} m/s in the along-track and 1×10^{-8} m/s in the cross-track direction
Ambiguity	Fixed for GPS, GLONASS, Galileo and BDS NONE GEO satellites
Satellite Maneuver	GPS/GLONASS/Galileo maneuver information from GFZ (https://semisys.gfz-potsdam.de/semisys/scripts/satellites/maneuver.php) (accessed on 25 July 2022) BDS/QZSS detected in real-time mode [32,33]
Ultrarapid orbit update interval	Hourly updated based on five-system POD processing within one hour
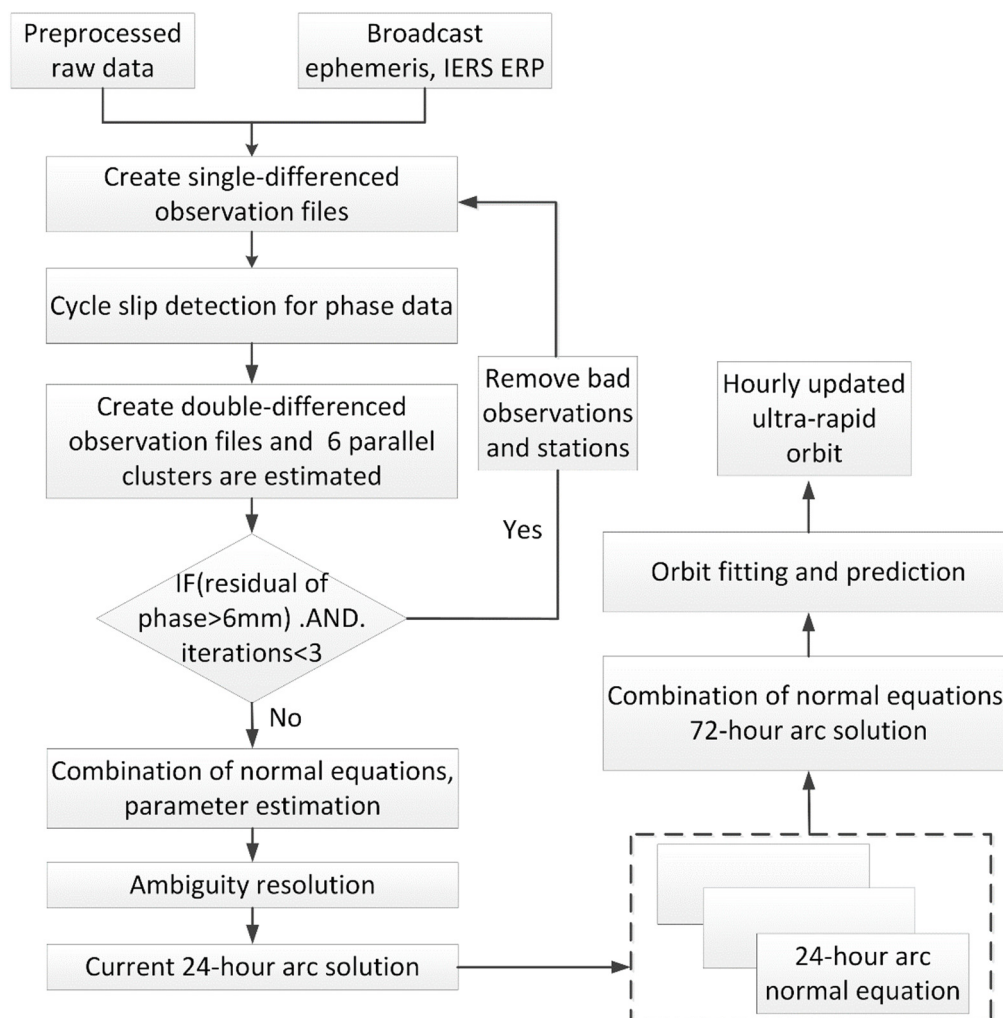
Figure 3. Flowchart of the procedure for real-time multi-GNSS POD.

Due to the lack of detailed surface geometric and optical information for GNSS satellites, the empirical CODE Orbit Model (ECOM1) [34], and its extended version ECOM2 [35], developed at the Center for Orbit Determination in Europe (CODE), are widely used in POD activities of IGS/iGMAS analysis centers. As to Galileo and BDS-3 satellites with the rectangular shapes, the most pronounced orbit errors caused by the inappropriate SRP model have been distinguished by the most recent researchers. A prior analytical SRP model for the Galileo constellation called the cuboid model or the DLR model has been established [36,37], which could be used a priori together with the empirical ECOM model to improve the Galileo orbit. Guo et al. [3], Wang et al. [38], Liu et al. [39] and Xia et al. [40] have also conducted some research on using an adjustable box-wing (ABW) model [41] a priori to strengthen the ECOM model. In this contribution, a priori cuboid model is introduced to enhance the five-parameter ECOM1 model for BDS-3 CAST (China Academy of Space Technology) satellites, BDS-3 SECM (Shanghai Engineering Center for Microsatellites, CAS) satellites as well as Galileo satellites. For BDS-3 satellite cuboid modelling, the parameters of the cuboid (a_C, a_S, a_A) are estimated and adjusted in the post-POD processing mode using the a priori cuboid+ECOM1 model, while ECOM1-only parameters are taken as the reference value, which is similar to Galileo cuboid modelling. All BDS-3 satellite metadata are obtained from China Satellite Navigation Office (CSNO) [42].

3. Results

Hourly updated ultrarapid orbits obtained in this contribution are assessed by comparing with GFZ final multi-GNSS orbits. Meanwhile, to investigate the hourly updated orbit boundary discontinuity, orbit boundary overlapping comparison has been carried out. Moreover, we assess the accuracy of BDS-3 satellite orbits which have been calculated with the a priori cuboid+ECOM1 model using SLR observations as an independent means.

### 3.1. Orbit Comparisons with GFZ Final Multi-GNSS Orbits

The satellite positions of two individual orbit products are compared in radial, along-tracking, cross-tracking (RAC) components and 1-D. The real-time POD is completed in one hour, and thus, the orbit within the second hour of each prediction in one day is extracted and merged to a complete 24 h orbit; then, the merged 24 h orbit is compared with GFZ's final daily multi-GNSS orbit. Finally, the mean RMS of each component for each satellite in all constellations from 1 June 2021 to 31 May 2022 is presented, and the results are shown in Figures 4–8 and listed in Tables 4–8. Meanwhile, time series of the 1-D for each constellation are illustrated in Figures 9–13. Statistics show that the mean 1-D RMS value over the RAC components is approximately 3.7 cm, 10.2 cm, 5.8 cm, 5.7 cm, 4.1 cm and 25.1 cm for GPS, BDS IGSOs, BDS MEOs, GLONASS, Galileo and QZSS NONE GEOs, respectively. As for the radial component, the mean RMS is approximately 1.7 cm, 5.8 cm, 3.4 cm 2.5 cm, 1.8 cm and 10.9 cm for GPS, BDS IGSOs, BDS MEOs, GLONASS, Galileo and QZSS NONE GEOs, respectively.

3.2. Hourly Orbit Boundary Discontinuities

To investigate the boundary discontinuities of the hourly updated ultrarapid orbits obtained in this contribution, the satellite positions from two adjacent hourly orbits at a specific epoch are compared to assess the orbits' internal accuracy. For each two adjacent hourly orbits shifted by one hour, the 2–3 h of current prediction and the 1–2 h of the adjacent prediction have been compared. Figure 14 illuminates the procedure of overlapping for two adjacent predictions of the 2 h arc.
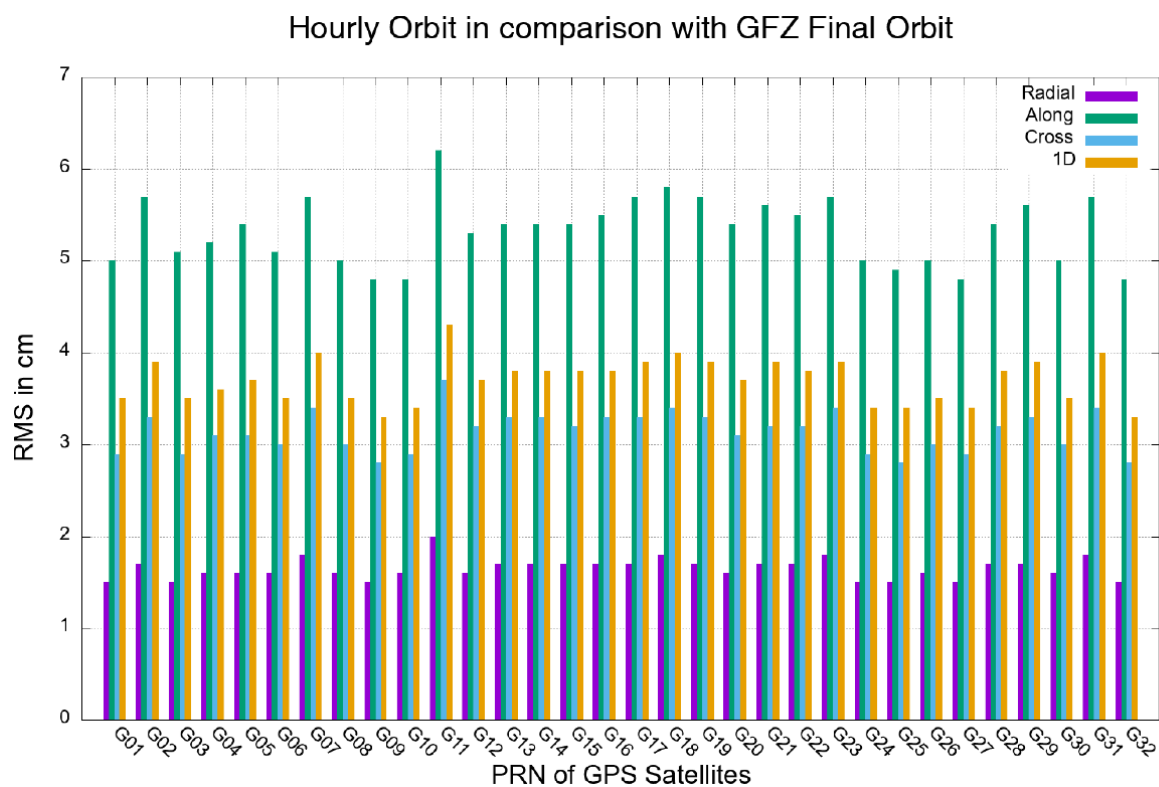
Figure 4. Mean RMS in the RAC components and 1-D of GPS satellites in comparison with GFZ final orbit.
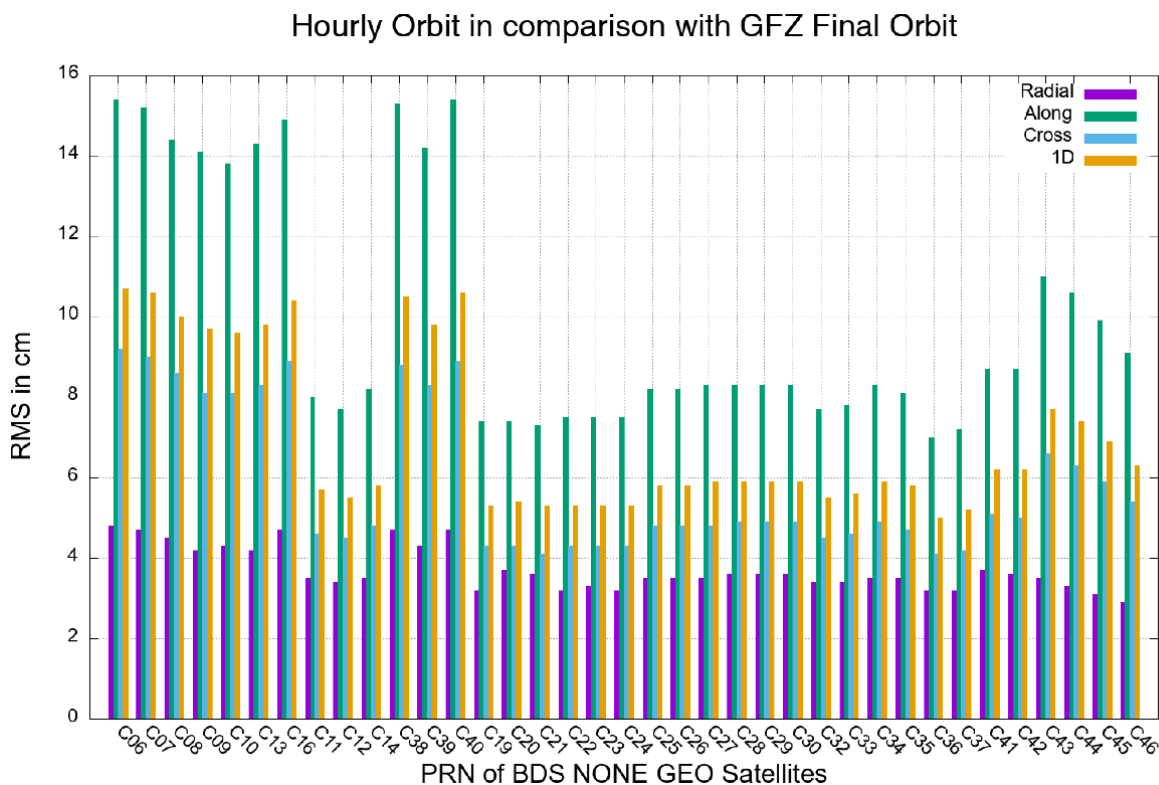
Figure 5. Mean RMS in the RAC components and 1-D of BDS NONE GEO satellites in comparison with GFZ final orbit.
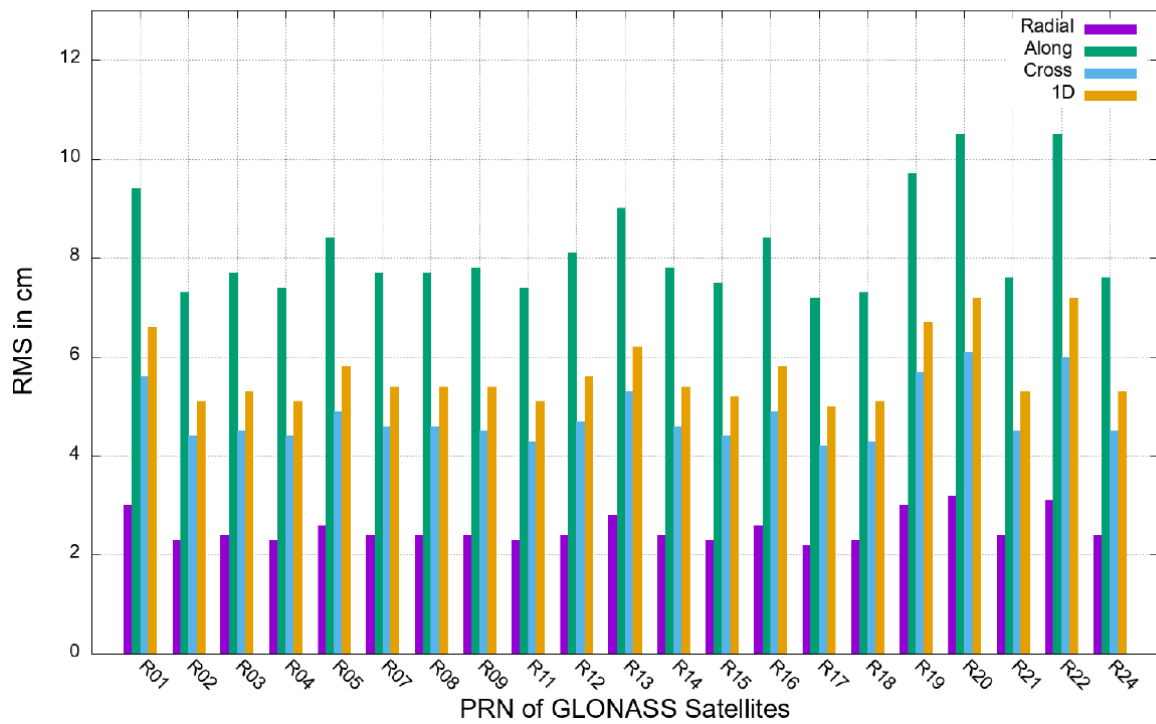
Hourly Orbit in comparison with GFZ Final Orbit

Figure 6. Mean RMS in the RAC components and 1-D of GLONASS satellites in comparison with GFZ final orbit.
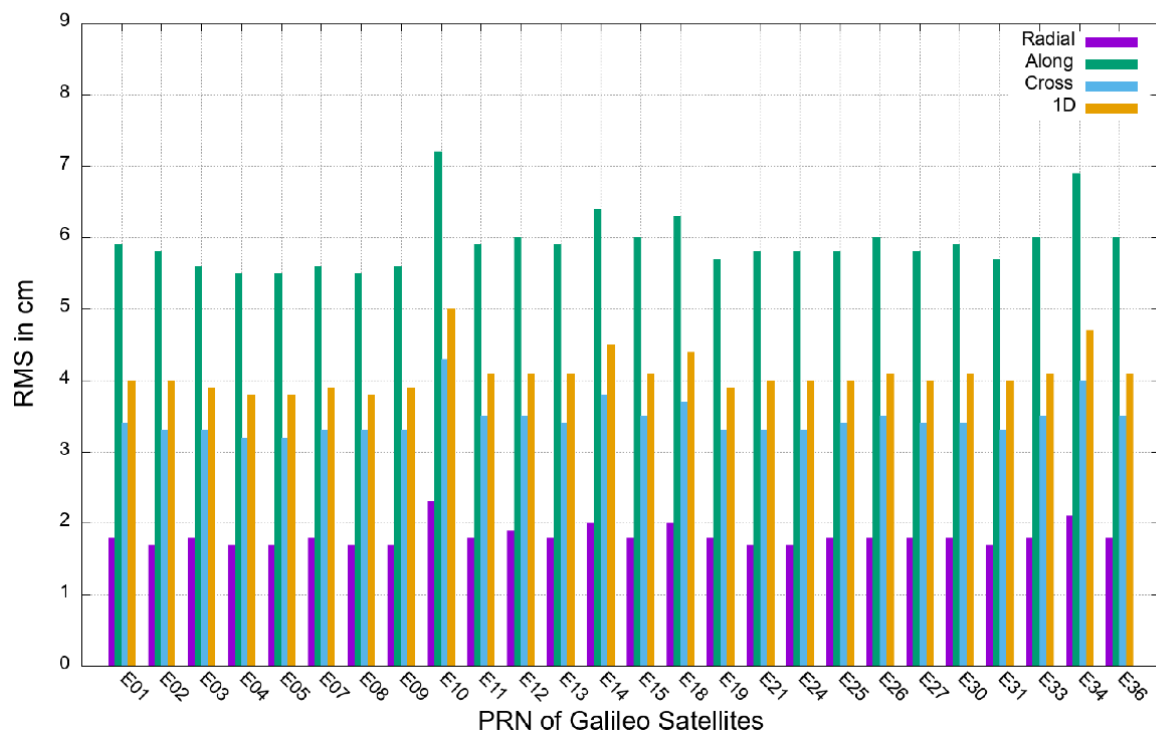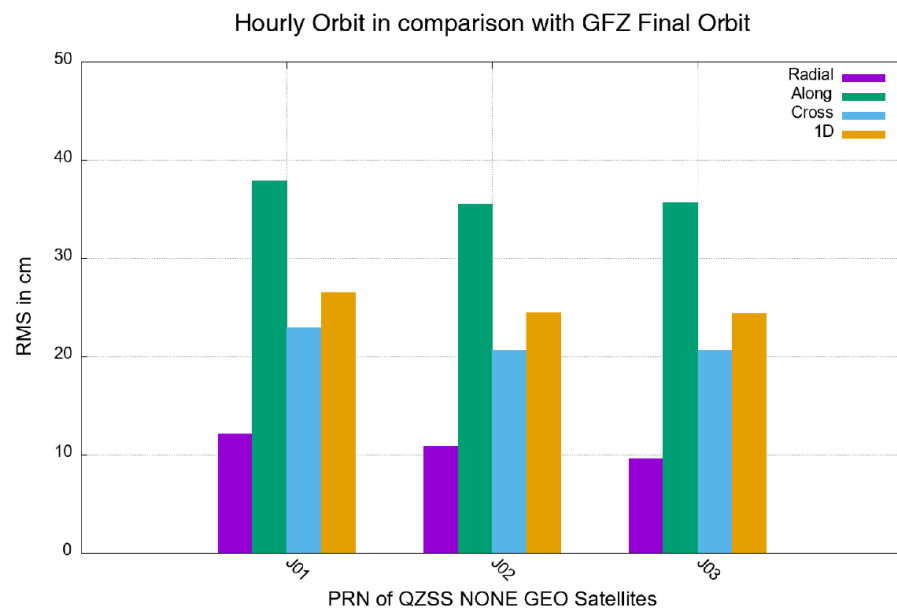
Hourly Orbit in comparison with GFZ Final Orbit

Figure 7. Mean RMS in the RAC components and 1-D of Galileo satellites in comparison with GFZ final orbit.

Figure 8. Mean RMS in the RAC components and 1-D of QZSS NONE GEO satellites in comparison with GFZ final orbit.

Table 4. Mean RMS value of GPS satellites in comparison with GFZ final orbit.

PRN of GPS	Radial (cm)	Along (cm)	Cross (cm)	1-D (cm)
G01	1.5	5.0	2.9	3.5
G02	1.7	5.7	3.3	3.9
G03	1.5	5.1	2.9	3.5
G04	1.6	5.2	3.1	3.6
G05	1.6	5.4	3.1	3.7
G06	1.6	5.1	3.0	3.5
G07	1.8	5.7	3.4	4.0
G08	1.6	5.0	3.0	3.5
G09	1.5	4.8	2.8	3.3
G10	1.6	4.8	2.9	3.4
G11	2.0	6.2	3.7	4.3
G12	1.6	5.3	3.2	3.7
G13	1.7	5.4	3.3	3.8
G14	1.7	5.4	3.3	3.8
G15	1.7	5.4	3.2	3.8
G16	1.7	5.5	3.3	3.8
G17	1.7	5.7	3.3	3.9
G18	1.8	5.8	3.4	4.0
G19	1.7	5.7	3.3	3.9
G20	1.6	5.4	3.1	3.7
G21	1.7	5.6	3.2	3.9
G22	1.7	5.5	3.2	3.8
G23	1.8	5.7	3.4	3.9
G24	1.5	5.0	2.9	3.4
G25	1.5	4.9	2.8	3.4
G26	1.6	5.0	3.0	3.5
G27	1.5	4.8	2.9	3.4
G28	1.7	5.4	3.2	3.8
G29	1.7	5.6	3.3	3.9
G30	1.6	5.0	3.0	3.5
G31	1.8	5.7	3.4	4.0
G32	1.5	4.8	2.8	3.3

Table 5. Mean RMS value of BDS NONE GEO satellites in comparison with GFZ final orbit.

PRN of BDS NONE GEOs	Radial (cm)	Along (cm)	Cross (cm)	1-D (cm)
BDS-2 IGSOs				
C06	4.8	15.4	9.2	10.7
C07	4.7	15.2	9.0	10.6
C08	4.5	14.4	8.6	10.0
C09	4.2	14.1	8.1	9.7
C10	4.3	13.8	8.1	9.6
C13	4.2	14.3	8.3	9.8
C16	4.7	14.9	8.9	10.4
BDS-2 MEOs				
C11	3.5	8.0	4.6	5.7
C12	3.4	7.7	4.5	5.5
C14	3.5	8.2	4.8	5.8
BDS-3 IGSOs				
C38	4.7	15.3	8.8	10.5
C39	4.3	14.2	8.3	9.8
C40	4.7	15.4	8.9	10.6
BDS-3 MEOs				
C19	3.2	7.4	4.3	5.3
C20	3.7	7.4	4.3	5.4
C21	3.6	7.3	4.1	5.3
C22	3.2	7.5	4.3	5.3
C23	3.3	7.5	4.3	5.3
C24	3.2	7.5	4.3	5.3
C25	3.5	8.2	4.8	5.8
C26	3.5	8.2	4.8	5.8
C27	3.5	8.3	4.8	5.9
C28	3.6	8.3	4.9	5.9
C29	3.6	8.3	4.9	5.9
C30	3.6	8.3	4.9	5.9
C32	3.4	7.7	4.5	5.5
C33	3.4	7.8	4.6	5.6
C34	3.5	8.3	4.9	5.9
C35	3.5	8.1	4.7	5.8
C36	3.2	7.0	4.1	5.0
C37	3.2	7.2	4.2	5.2
C41	3.7	8.7	5.1	6.2
C42	3.6	8.7	5.0	6.2
C43	3.5	11.0	6.6	7.7
C44	3.3	10.6	6.3	7.4
C45	3.1	9.9	5.9	6.9
C46	2.9	9.1	5.4	6.3

Table 6. Mean RMS value of GLONASS satellites in comparison with GFZ final orbit.

PRN of GLONASS	Radial (cm)	Along (cm)	Cross (cm)	1-D (cm)
R01	3.0	9.4	5.6	6.6
R02	2.3	7.3	4.4	5.1
R03	2.4	7.7	4.5	5.3
R04	2.3	7.4	4.4	5.1
R05	2.6	8.4	4.9	5.8
R07	2.4	7.7	4.6	5.4

Table 6. *Cont.*

PRN of GLONASS	Radial (cm)	Along (cm)	Cross (cm)	1-D (cm)
R08	2.4	7.7	4.6	5.4
R09	2.4	7.8	4.5	5.4
R11	2.3	7.4	4.3	5.1
R12	2.4	8.1	4.7	5.6
R13	2.8	9.0	5.3	6.2
R14	2.4	7.8	4.6	5.4
R15	2.3	7.5	4.4	5.2
R16	2.6	8.4	4.9	5.8
R17	2.2	7.2	4.2	5.0
R18	2.3	7.3	4.3	5.1
R19	3.0	9.7	5.7	6.7
R20	3.2	10.5	6.1	7.2
R21	2.4	7.6	4.5	5.3
R22	3.1	10.5	6.0	7.2
R24	2.4	7.6	4.5	5.3

Table 7. Mean RMS value of Galileo satellites in comparison with GFZ final orbit.

PRN of Galileo	Radial (cm)	Along (cm)	Cross (cm)	1-D (cm)
E01	1.8	5.9	3.4	4.0
E02	1.7	5.8	3.3	4.0
E03	1.8	5.6	3.3	3.9
E04	1.7	5.5	3.2	3.8
E05	1.7	5.5	3.2	3.8
E07	1.8	5.6	3.3	3.9
E08	1.7	5.5	3.3	3.8
E09	1.7	5.6	3.3	3.9
E10	2.3	7.2	4.3	5.0
E11	1.8	5.9	3.5	4.1
E12	1.9	6.0	3.5	4.1
E13	1.8	5.9	3.4	4.1
E14	2.0	6.4	3.8	4.5
E15	1.8	6.0	3.5	4.1
E18	2.0	6.3	3.7	4.4
E19	1.8	5.7	3.3	3.9
E21	1.7	5.8	3.3	4.0
E24	1.7	5.8	3.3	4.0
E25	1.8	5.8	3.4	4.0
E26	1.8	6.0	3.5	4.1
E27	1.8	5.8	3.4	4.0
E30	1.8	5.9	3.4	4.1
E31	1.7	5.7	3.3	4.0
E33	1.8	6.0	3.5	4.1
E34	2.1	6.9	4.0	4.7
E36	1.8	6.0	3.5	4.1

Table 8. Mean RMS value of QZSS NONE GEO satellites in comparison with GFZ final orbit.

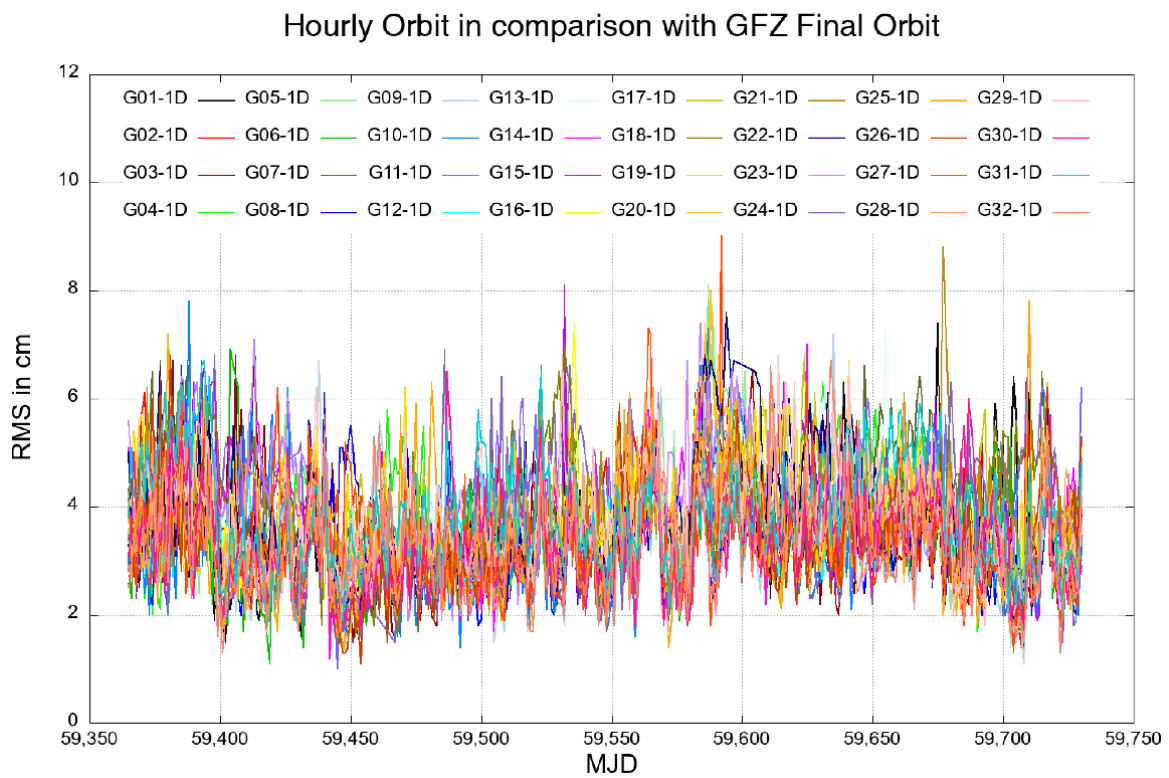| PRN of QZSS NONE GEOs	Radial (cm)	Along (cm)	Cross (cm)	1-D (cm)
J01	12.1	37.9	22.9	26.5
J02	10.9	35.5	20.6	24.5
J03	9.6	35.7	20.6	24.4

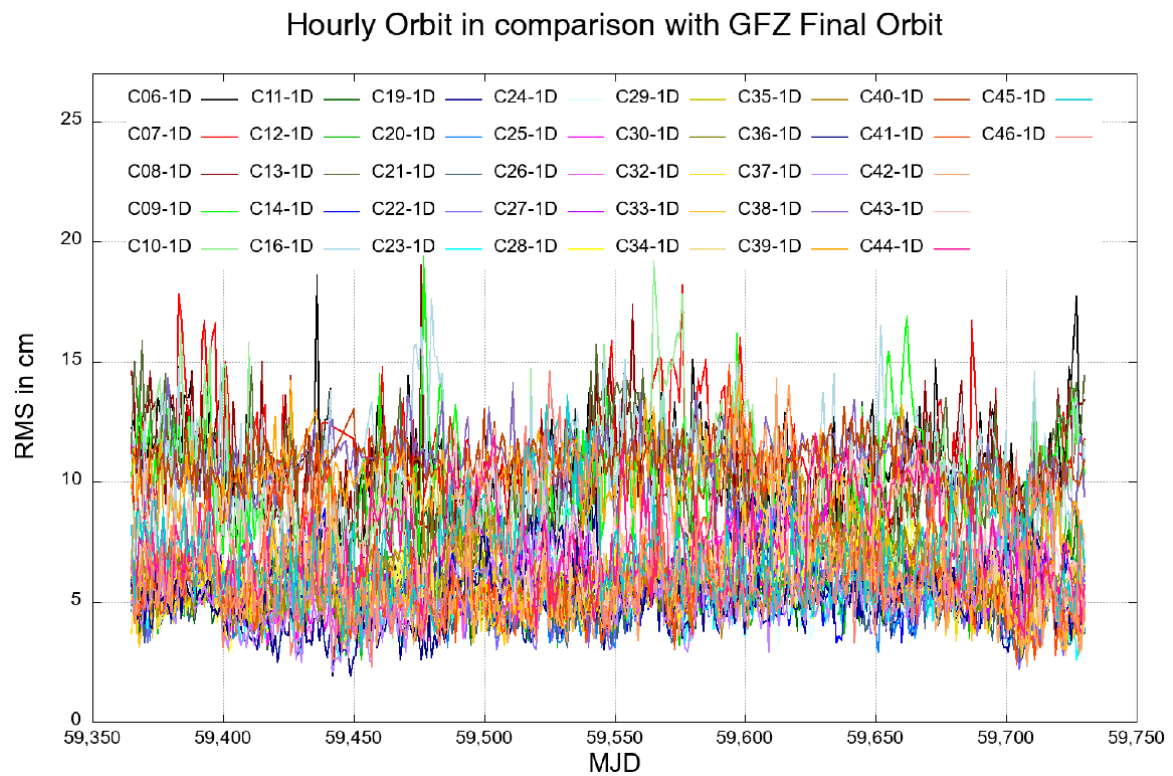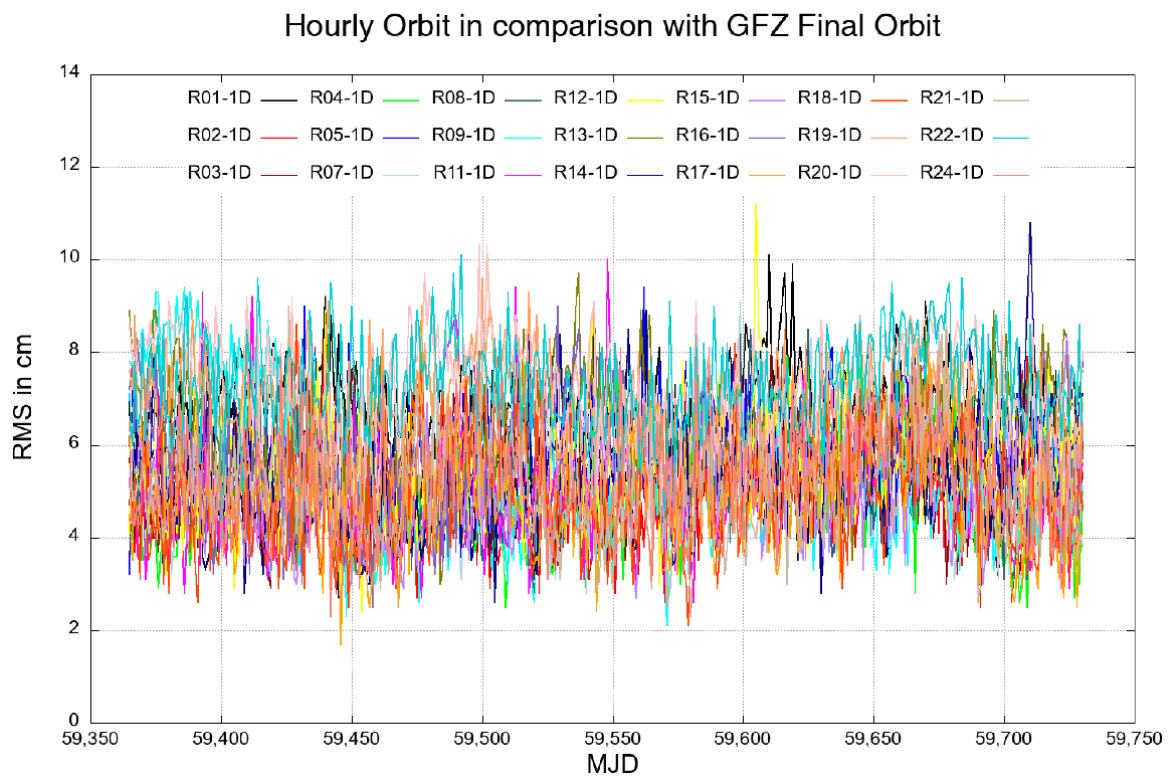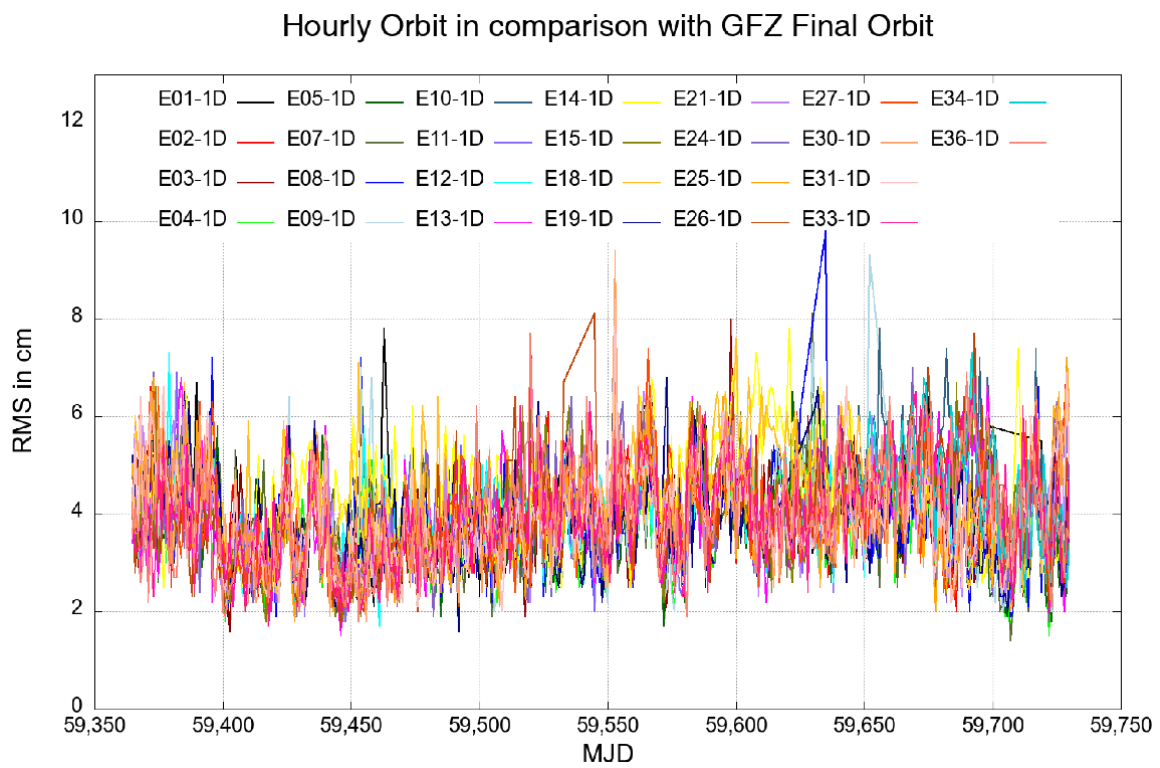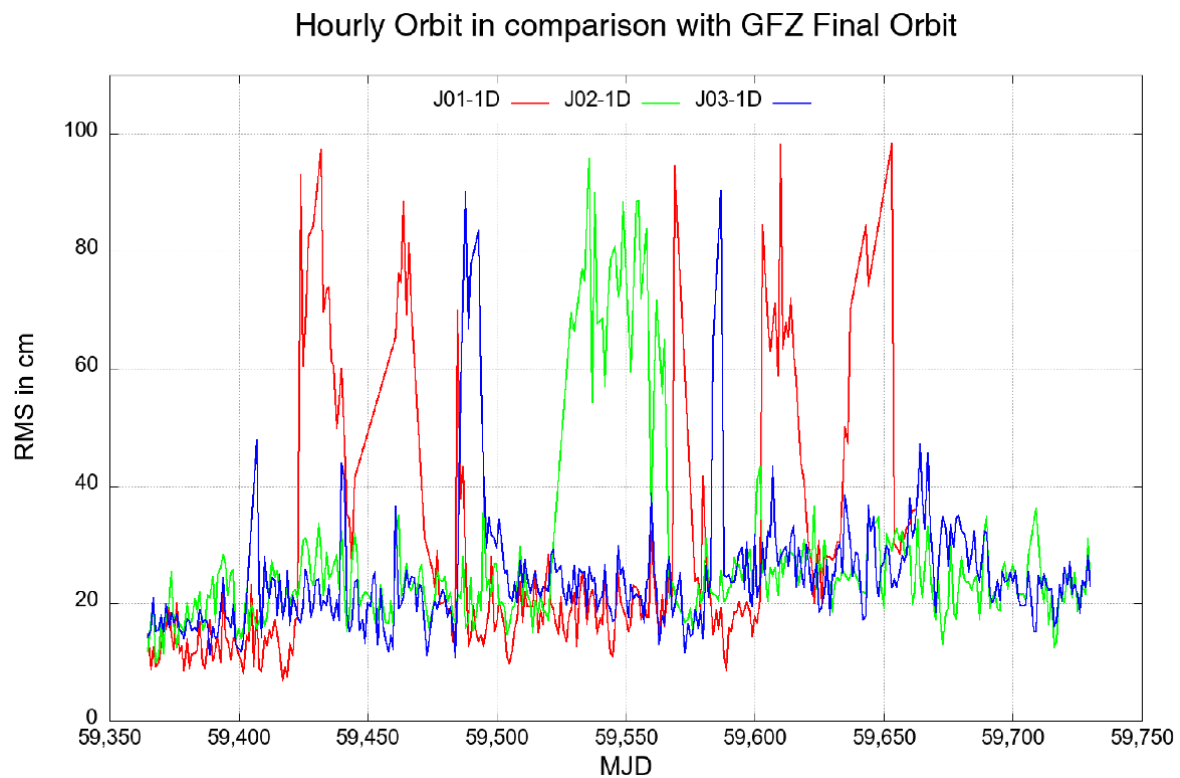**Figure 9.** Time series in 1-D of GPS satellites compared with GFZ final orbit.

**Figure 10.** Time series in 1-D of BDS NONE GEO satellites compared with GFZ final orbit.

Figure 11. Time series in 1-D of GLONASS satellites compared with GFZ final orbit.

Figure 12. Time series in 1-D of Galileo satellites compared with GFZ final orbit.

Hourly Orbit in comparison with GFZ Final Orbit

Figure 13. Time series in 1-D of QZSS NONE GEO satellites compared with GFZ final orbit.
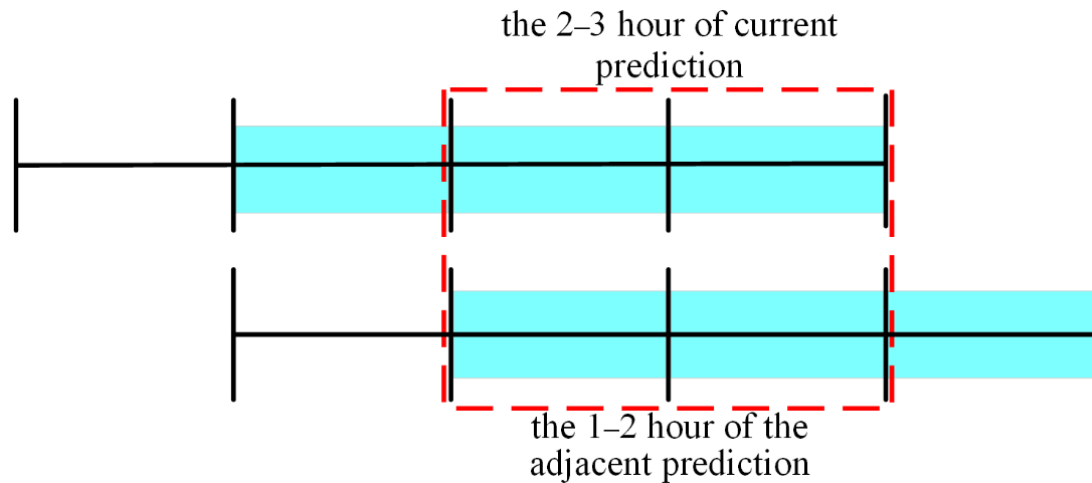
Figure 14. A 2–h arc overlap comparison of two adjacent ultrarapid orbits.

The hourly ultrarapid orbit of GPS Week 2211 (from 22 May 2022 to 28 May 2022) are processed, and the mean RMS values of 2 h overlapping in the RAC components and 1-D for each constellation are demonstrated in Figures 15–19. As seen in Figures 15–19, the mean 1-D RMS value over the RAC components is approximately 1.6 cm, 6.9 cm, 3.2 cm, 2.7 cm, 1.8 cm and 22.2 cm for GPS, BDS IGSOs, BDS MEOs, GLONASS, Galileo and QZSS NONE GEOs, respectively. As for the radial component, the mean RMS is approximately 0.7 cm, 3.1 cm, 1.5 cm, 1.2 cm, 0.8 cm and 8.2 cm for GPS, BDS IGSOs, BDS MEOs, GLONASS, Galileo and QZSS NONE GEOs, respectively. The results of the hourly orbit boundary discontinuities for BDS and QZSS indicate that there still exist some mismodeled or unmodeled force errors which should be further investigated.
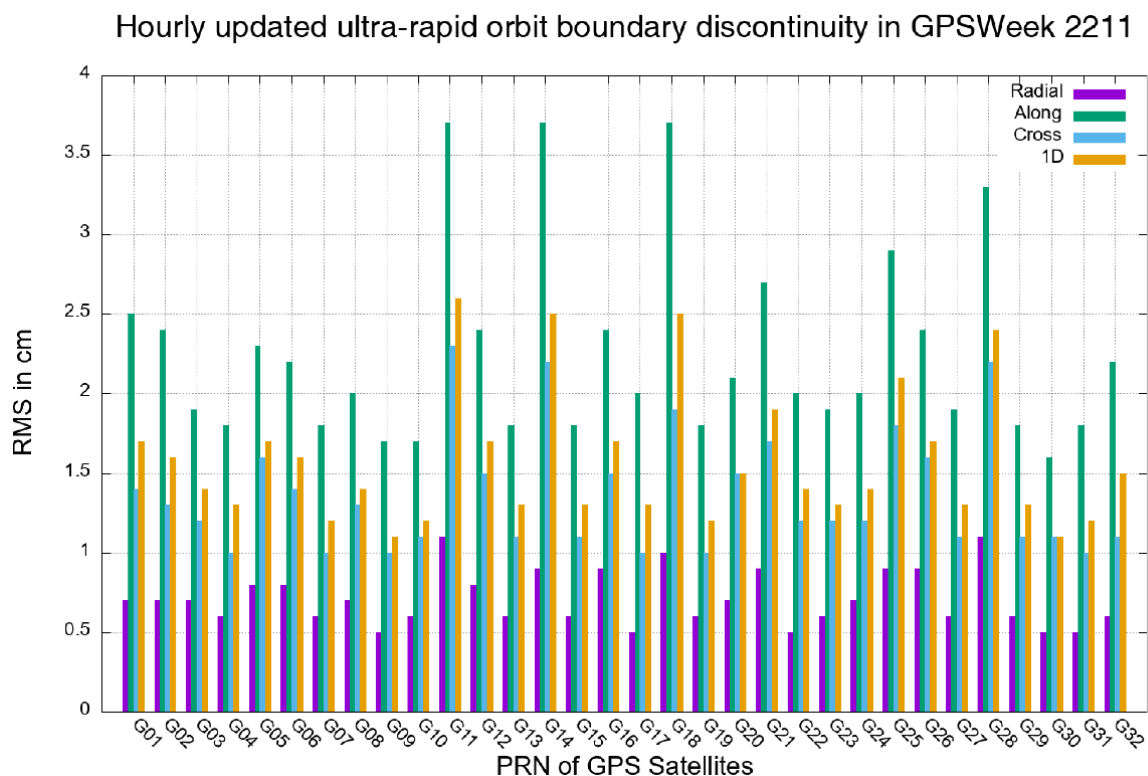
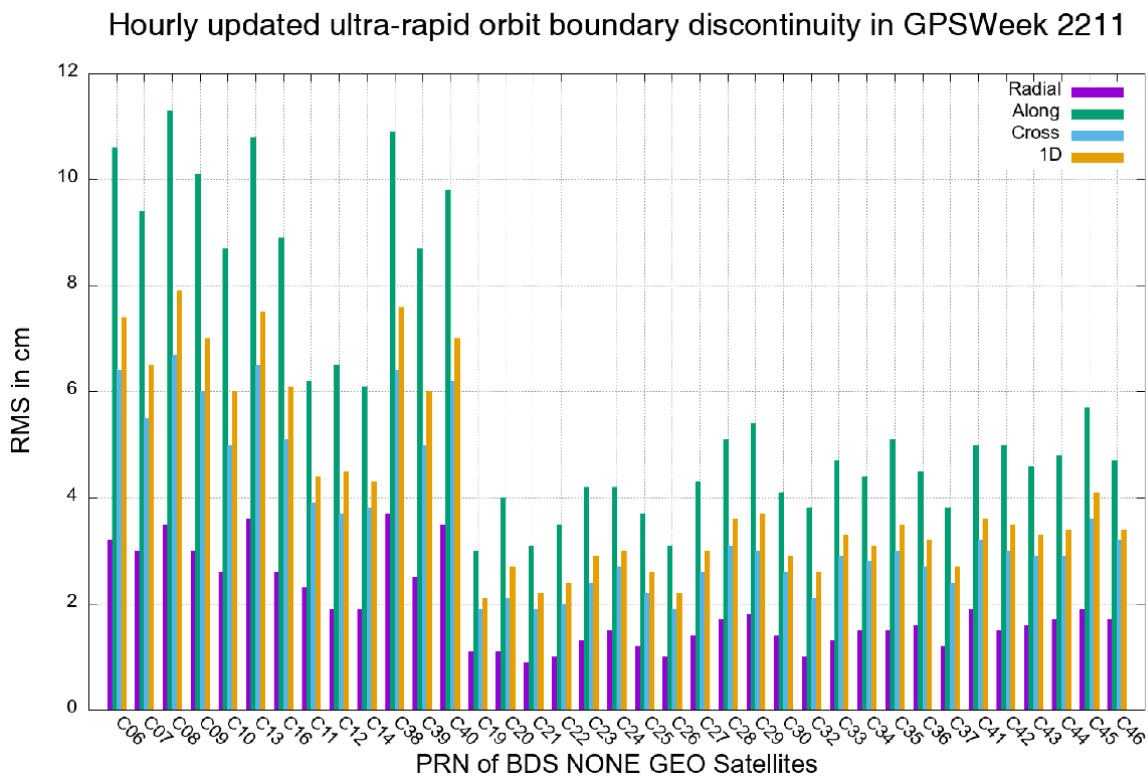**Figure 15.** Mean RMS of overlapping in the RAC components and 1-D of GPS satellites.

Figure 16. Mean RMS of overlapping in the RAC components and 1-D of BDS NONE GEO satellites.

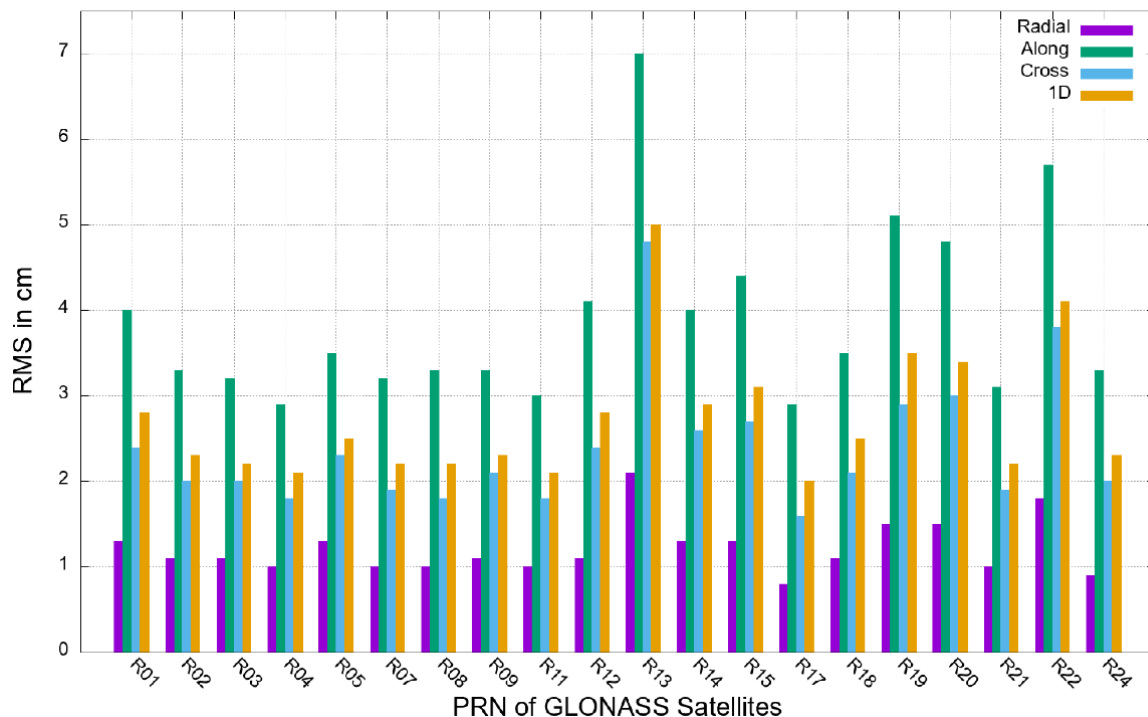Hourly updated ultra-rapid orbit boundary discontinuity in GPSWeek 2211

Figure 17. Mean RMS of overlapping in the RAC components and 1-D of GLONASS satellites.

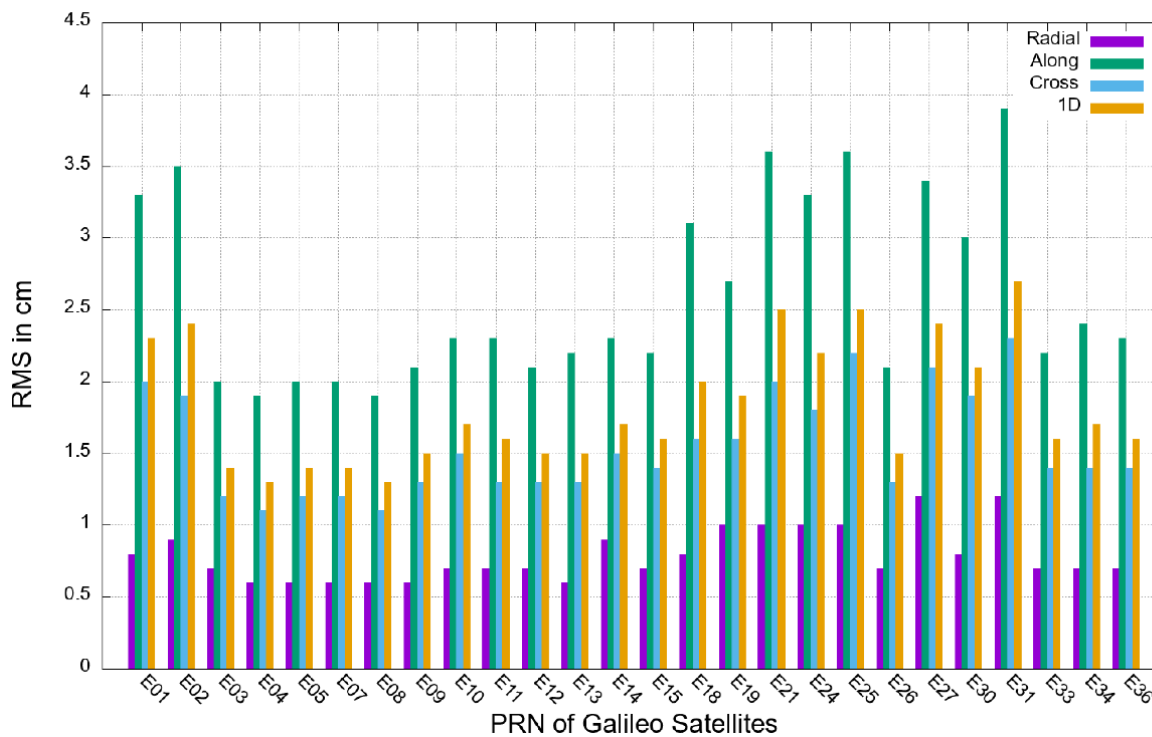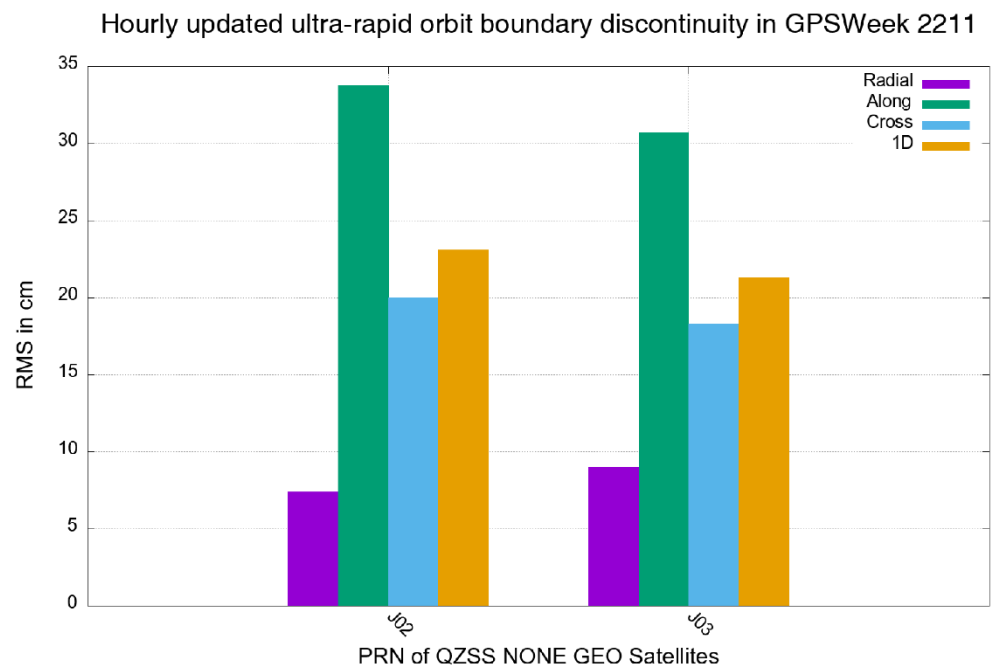Hourly updated ultra-rapid orbit boundary discontinuity in GPSWeek 2211

**Figure 18.** Mean RMS of overlapping in the RAC components and 1-D of Galileo satellites.

Figure 19. Mean RMS of overlapping in the RAC components and 1-D of QZSS NONE GEO satellites.

3.3. SLR Residuals

To further investigate the effect of the a priori cuboid+ECOM1 model applied for BDS-3 satellites, SLRhas been used to investigate the orbits. BDS-3 C20, C21, C29 and C30 are the current ongoing missions of the International Laser Ranging Service (ILRS) [43], and the SLR range observations can be downloaded from the ILRS EUROLAS Data Center (EDC). The system eccentricities and station coordinates have been obtained through https://cddis.nasa.gov/archive/slr/slrocc/ecc_une.snx (accessed on 25 July 2022) and https://cddis.nasa.gov/archive/slr/products/pos+eop (accessed on 25 July 2022). BDS-3 satellites' retro-reflector offsets are obtained from CSNO. The SLR normal points (NP) from 1 June 2021 to 31 May 2022 collected by 15 SLR stations (Yarragadee, Changchun, Herstmonceux, Mount Stromlo, Beijing, Monument P, Graz, Shanghai, Grasse, Papeete, Potsdam, Zimmerwald, Simeiz, Katzively and Greenbelt) are processed. Meanwhile, three BDS-2 IGSOs (C08, C10, C13) and one BDS-2 MEO (C11) are also validated. The statistics of the SLR validation for BDS-3 and BDS-2 satellites are demonstrated in Table 9 and shown in Figures 20 and 21. The result coincide with the radial part of the external orbit comparison. The mean RMS value for BDS-3 four MEOs is approximately 4.53 cm, and the biases are approximately −4 cm and 3 cm for BDS-3 SECM and CAST MEOs, respectively. The mean RMS value for BDS-2 four satellites is approximately 4.73 cm, and the biases are approximately 1–2 cm.

Table 9. Biases and mean RMS of SLR validation of BDS satellites.

PRN of BDS-3	AVE (cm)	RMS (cm)
M2, C20 (CAST)	3.29	4.39
M3, C21 (CAST)	3.08	4.61
M9, C29 (SECM)	−4.09	4.64
M10, C30 (SECM)	−3.93	4.48
PRN of BDS-2	**AVE (cm)**	**RMS (cm)**
I3, C08 (IGSO)	0.99	4.76
I5, C10 (IGSO)	1.95	4.73
I6, C13 (IGSO)	1.13	4.74
M3, C11 (MEO)	1.29	4.67
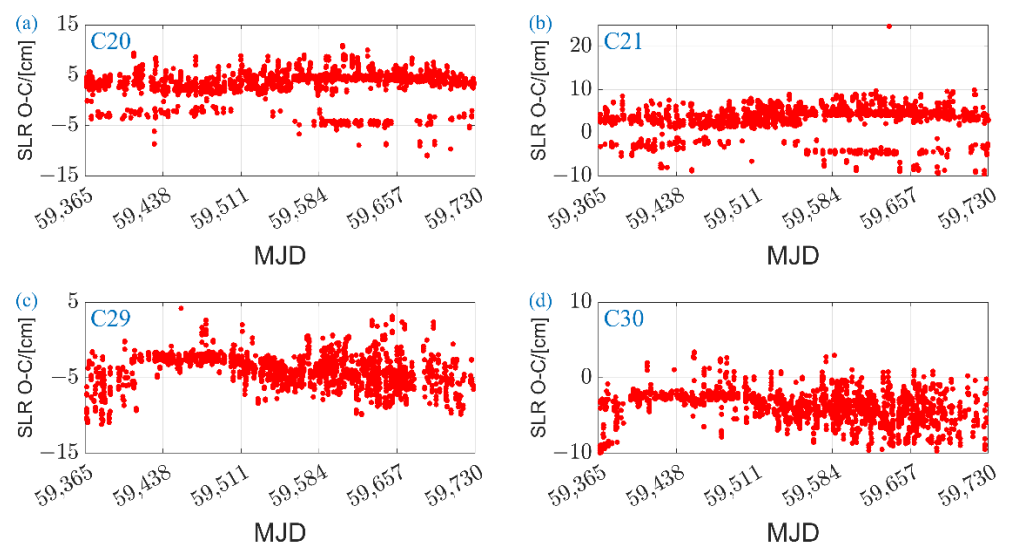
Figure 20. SLR validation results of BDS-3 (**a**) C20 (M2), (**b**) C21 (M3), (**c**) C29 (M9) and (**d**) C30 (M10) orbits.
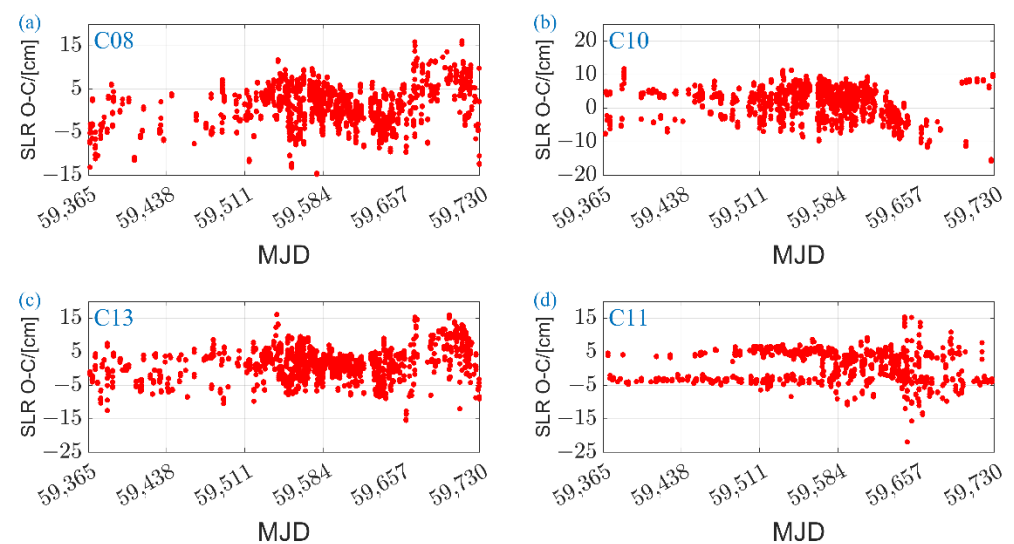
Figure 21. SLR validation results of BDS-2 (**a**) C08 (I3), (**b**) C10 (I5), (**c**) C13 (I6) and (**d**) C11(M3) orbits.

4. Discussion

In the literature, many studies analyzed the 6 h and 3 h updated GNSS satellite orbit and its application, and few orbit products contain the full constellation of Galileo, BDS and QZSS NONE GEOs. Disadvantages about accuracy, latency and stability have still been recognized in recent research works using the predicted half of IGS ultrarapid ephemerides (6 h update interval and 3 h latency) for real-time applications. A strategy of real-time multi-GNSS orbit determination via hourly update is proposed in this contribution. With the station-clustered and parallel processing method, POD of multi-GNSS can be conducted within one hour, and thus, hourly updated orbit is achievable using cloud servers. By comparing with GFZ final orbits, orbit boundary discontinuity investigation and SLR validation, we analyzed the performance of our orbit.

Comparison with GFZ final multi-GNSS orbits show improvement of our GPS orbit with respect to the predicted half of IGS ultrarapid GPS satellite ephemerides with a nominal accuracy of 5 cm (1-D mean RMS). It should be noted that the accuracy of the Galileo constellation is almost equal to that of GPS not only in external orbit comparison but also in orbit boundary discontinuity investigation. For BDS, BDS IGSOs have larger

RMS values than MEOs, mainly due to the observational geometry. It should also be noted that accuracy of BDS MEOs is almost equal to that of the GLONASS constellation. Due to limited observational geometry and limited tracking stations, the accuracy of the QZSS constellation is worse than that of other constellations in external orbit comparison, which has also been recognized in a further orbit boundary discontinuity assessment. As to our investigation, another possible cause is some mismodeled or unmodeled force errors such as the solar pressure model (SRP) and the inappropriate satellite attitude model, which should be further investigated. SLR validation results show that the BDS satellite orbit radial error is in good agreement with the external orbit comparison. The a priori cuboid + ECOM1 model helps BDS-3 satellites achieve subequal accuracy with respect to BDS-2, whereas the average value of SLR validation indicates that further studies on empirical SRP modelling for BDS-3 satellites are still essential.

5. Conclusions

This contribution summarizes the specific five-system, real-time POD strategy based on the hourly updated ultrarapid orbit prediction method; particularly, an a priori cuboid model is introduced to enhance the five-parameter ECOM1 model for BDS-3 satellites. One year of observations from 21 iGMAS stations and 100 IGS/MGEX stations are processed for POD of multi-GNSS. External orbit comparison, hourly orbit boundary discontinuities and SLR validations are conducted, and it is shown that the mean 1-D RMS values with comparison to the GFZ final multi-GNSS orbits are approximately 3.7 cm, 10.2 cm, 5.8 cm, 5.7 cm, 4.1 cm and 25.1 cm for GPS, BDS IGSOs, BDS MEOs, GLONASS, Galileo and QZSS NONE GEOs, respectively. It is also shown that the mean 1-D RMS values of the hourly updated ultrarapid orbit boundary overlapping comparison are approximately 1.6 cm, 6.9 cm, 3.2 cm, 2.7 cm, 1.8 cm and 22.2 cm for GPS, BDS IGSOs, BDS MEOs, GLONASS, Galileo and QZSS NONE GEOs, respectively. The results of the hourly orbit boundary discontinuities for BDS and QZSS indicate that there still exist some mismodeled or unmodeled force errors which should be further investigated. As to the SLR validation, the mean RMS value for the four MEOs of BDS-3 is approximately 4.53 cm, and the biases are approximately -4 cm and 3 cm for BDS-3 SECM and CAST MEOs, respectively. The mean RMS value of the BDS-2 four satellites is approximately 4.73 cm, and the biases are approximately 1–2 cm.

References

1. Yang, Y.; Mao, Y.; Sun, B. Basic performance and future developments of BeiDou global navigation satellite system. *Satell. Navig.* **2020**, *1*, 1. [CrossRef]
2. Yang, Y.; Xu, Y.; Li, J.; Yang, C. Progress and performance evaluation of BeiDou global navigation satellite system: Data analysis based on BDS-3 demonstration system. *Sci. China Earth Sci.* **2018**, *61*, 614–624. [CrossRef]
3. Guo, J. The Impacts of Attitude, Solar Radiation and Function Model on Precise Orbit Determination for GNSS Satellites. Ph.D. Thesis, Wuhan University, Wuhan, China, 2014.
4. Prange, L.; Orliac, E.; Dach, R.; Arnold, D.; Beutler, G.; Schaer, S.; Jäggi, A. CODE's five-system orbit and clock solution—the challenges of multi-GNSS data analysis. *J. Geod.* **2017**, *91*, 345–360. [CrossRef]
5. Prange, L.; Villiger, A.; Sidorov, D.; Schaer, S.; Beutler, G.; Dach, R.; Jäggi, A. Overview of CODE's MGEX solution with the focus on Galileo. *Adv. Space Res.* **2020**, *66*, 2786–2798. [CrossRef]
6. Zhang, B.; Chen, Y.; Yuan, Y. PPP-RTK based on undifferenced and uncombined observations: Theoretical and practical aspects. *J. Geod.* **2019**, *93*, 1011–1024. [CrossRef]
7. Liu, T.; Zhang, B.; Yuan, Y.; Li, M. Real-Time Precise Point Positioning (RTPPP) with raw observations and its application in real-time regional ionospheric VTEC modeling. *J. Geod.* **2018**, *92*, 1267–1283. [CrossRef]
8. Zha, J.; Zhang, B.; Liu, T.; Hou, P. Ionosphere-weighted undifferenced and uncombined PPP-RTK: Theoretical models and experimental results. *GPS Solut.* **2021**, *25*, 135. [CrossRef]
9. Ai, Q.; Zhang, B.; Yuan, Y.; Xu, T.; Chen, Y.; Tan, B. Evaluation and mitigation of the influence of pseudorange biases on GNSS satellite clock offset estimation. *Measurement* **2022**, *193*, 111015. [CrossRef]
10. Ai, Q.; Yuan, Y.; Zhang, B.; Xu, T.; Chen, Y. Refining GPS/GLONASS Satellite Clock Offset Estimation in the Presence of Pseudo-Range Inter-Channel Biases. *Remote Sens.* **2020**, *12*, 1821. [CrossRef]
11. Zhang, B.; Teunissen, P.J. Characterization of multi-GNSS between-receiver differential code biases using zero and short baselines. *Sci. Bull.* **2015**, *60*, 1840–1849. [CrossRef]
12. Zhang, B.; Teunissen, P.J.; Odijk, D. A novel un-differenced PPP-RTK concept. *J. Navig.* **2011**, *64*, S180–S191. [CrossRef]
13. Bertiger, W.; Bar-Sever, Y.; Dorsey, A.; Haines, B.; Harvey, N.; Hemberger, D.; Heflin, M.; Lu, W.; Miller, M.; Moore, A.W. GipsyX/RTGx, a new tool set for space geodetic operations and research. *Adv. Space Res.* **2020**, *66*, 469–489. [CrossRef]
14. Zhang, Q.; Moore, P.; Hanley, J.; Martin, S. Auto-BAHN: Software for near real-time GPS orbit and clock computations. *Adv. Space Res.* **2007**, *39*, 1531–1538. [CrossRef]
15. Kazmierski, K.; Sośnica, K.; Hadas, T. Quality assessment of multi-GNSS orbits and clocks for real-time precise point positioning. *Gps Solut.* **2018**, *22*, 11. [CrossRef]
16. Zhang, S.; Du, S.; Li, W.; Wang, G. Evaluation of the GPS precise orbit and clock corrections from MADOCA real-time products. *Sensors* **2019**, *19*, 2580. [CrossRef]
17. Dai, X.; Lou, Y.; Dai, Z.; Qing, Y.; Li, M.; Shi, C. Real-time precise orbit determination for BDS satellites using the square root information filter. *GPS Solut.* **2019**, *23*, 45. [CrossRef]
18. Duan, B.; Hugentobler, U.; Chen, J.; Selmke, I.; Wang, J. Prediction versus real-time orbit determination for GNSS satellites. *GPS Solut.* **2019**, *23*, 39. [CrossRef]
19. Montenbruck, O.; Steigenberger, P.; Prange, L.; Deng, Z.; Zhao, Q.; Perosanz, F.; Romero, I.; Noll, C.; Stürze, A.; Weber, G. The Multi-GNSS Experiment (MGEX) of the International GNSS Service (IGS)–achievements, prospects and challenges. *Adv. Space Res.* **2017**, *59*, 1671–1697. [CrossRef]
20. Jiao, W. International GNSS Monitoring and Assessment System (iGMAS) and latest progress. In Proceedings of the China Satellite Navigation Conference (CSNC), Nanjing, China, 21–23 May 2014.
21. Deng, Z.; Fritsche, M.; Nischan, T.; Bradke, M. *Multi-GNSS Ultra Rapid Orbit-, Clock-& EOP Product Series, GFZ Data Services*; Technical Report; 2016.
22. Guo, J.; Xu, X.; Zhao, Q.; Liu, J. Precise orbit determination for quad-constellation satellites at Wuhan University: Strategy, result validation, and comparison. *J. Geod.* **2016**, *90*, 143–159. [CrossRef]
23. Kuang, K.; Zhang, S.; Li, J. Real-time GPS satellite orbit and clock estimation based on OpenMP. *Adv. Space Res.* **2019**, *63*, 2378–2386. [CrossRef]
24. Li, X.; Ge, M.; Dai, X.; Ren, X.; Fritsche, M.; Wickert, J.; Schuh, H. Accuracy and reliability of multi-GNSS real-time precise positioning: GPS, GLONASS, BeiDou, and Galileo. *J. Geod.* **2015**, *89*, 607–635. [CrossRef]
25. Shi, C.; Zhao, Q.; Li, M.; Tang, W.; Hu, Z.; Lou, Y.; Zhang, H.; Niu, X.; Liu, J. Precise orbit determination of Beidou Satellites with precise positioning. *Sci. China Earth Sci.* **2012**, *55*, 1079–1086. [CrossRef]
26. Li, X.; Chen, X.; Ge, M.; Schuh, H. Improving multi-GNSS ultra-rapid orbit determination for real-time precise point positioning. *J. Geod.* **2019**, *93*, 45–64. [CrossRef]
27. Choi, K.K.; Ray, J.; Griffiths, J.; Bae, T.-S. Evaluation of GPS orbit prediction strategies for the IGS Ultra-rapid products. *GPS Solut.* **2013**, *17*, 403–412. [CrossRef]
28. Hadas, T.; Bosy, J. IGS RTS precise orbits and clocks verification and quality degradation over time. *GPS Solut.* **2015**, *19*, 93–105. [CrossRef]
29. Rülke, A.; Agrotis, L.; Enderle, W.; MacLeod, K. IGS real time service–status, future tasks and limitations. In *Proceedings of the IGS Workshop, Sydney, Australia, 8–12 February 2016*; Federal Agency for Cartography and Geodesy: Frankfurt, Germany, 2016.

30. Montenbruck, O.; Schmid, R.; Mercier, F.; Steigenberger, P.; Noll, C.; Fatkulin, R.; Kogure, S.; Ganeshan, A.S. GNSS satellite geometry and attitude models. *Adv. Space Res.* **2015**, *56*, 1015–1029. [CrossRef]

31. Petit, G.; Luzum, B. *IERS Conventions*; Verlag des Bundesamts für Kartographie und Geodäsie: Frankfurt, Germany, 2010; ISBN 3-89888-989-6.

32. Song, W.; Li, C.; Dai, X.; Lou, Y.; Xu, Y. BDS near real-time maneuver detection based on triple-differenced phase observations. *Adv. Space Res.* **2022**, *69*, 3032–3043. [CrossRef]

33. Ye, F.; Yuan, Y.; Tan, B.; Ou, J. A robust method to detect BeiDou navigation satellite system orbit maneuvering/anomalies and its applications to precise orbit determination. *Sensors* **2017**, *17*, 1129. [CrossRef]

34. Beutler, G.; Brockmann, E.; Gurtner, W.; Hugentobler, U.; Mervart, L.; Rothacher, M.; Verdun, A. Extended orbit modeling techniques at the CODE processing center of the international GPS service for geodynamics (IGS): Theory and initial results. *Manuscr. Geod.* **1994**, *19*, 367–386.

35. Arnold, D.; Meindl, M.; Beutler, G.; Dach, R.; Schaer, S.; Lutz, S.; Prange, L.; Sośnica, K.; Mervart, L.; Jäggi, A. CODE's new solar radiation pressure model for GNSS orbit determination. *J. Geod.* **2015**, *89*, 775–791. [CrossRef]

36. Montenbruck, O.; Steigenberger, P.; Hugentobler, U. Enhanced solar radiation pressure modeling for Galileo satellites. *J. Geod.* **2015**, *89*, 283–297. [CrossRef]

37. Sidorov, D.; Dach, R.; Polle, B.; Prange, L.; Jäggi, A. Adopting the empirical CODE orbit model to Galileo satellites. *Adv. Space Res.* **2020**, *66*, 2799–2811. [CrossRef]

38. Wang, C. Solar Radiation Pressure Modelling for BeiDou Navigation Satellites. Ph.D. Thesis, Wuhan University, Wuhan, China, 2019.

39. Liu, Y.; Liu, Y.; Tian, Z.; Dai, X.; Qing, Y.; Li, M. Impact of ECOM Solar Radiation Pressure Models on Multi-GNSS Ultra-Rapid Orbit Determination. *Remote Sens.* **2019**, *11*, 3024. [CrossRef]

40. Xia, F.; Ye, S.; Chen, D.; Tang, L.; Wang, C.; Ge, M.; Neitzel, F. Advancing the Solar Radiation Pressure Model for BeiDou-3 IGSO Satellites. *Remote Sens.* **2022**, *14*, 1460. [CrossRef]

41. Rodriguez-Solano, C.; Hugentobler, U.; Steigenberger, P. Adjustable box-wing model for solar radiation pressure impacting GPS satellites. *Adv. Space Res.* **2012**, *49*, 1113–1128. [CrossRef]

42. China Satellite Navigation Office. BeiDou Satellite Metadata. Available online: http://en.beidou.gov.cn/SYSTEMS/Officialdocument/201912/P020200323536298695483.zip (accessed on 8 March 2021).

43. Pearlman, M.R.; Degnan, J.J.; Bosworth, J.M. The international laser ranging service. *Adv. Space Res.* **2002**, *30*, 135. [CrossRef]